

# Realization of polarization evolution on higher-order Poincaré sphere with metasurface

Yachao Liu,<sup>1</sup> Xiaohui Ling,<sup>1</sup> Xunong Yi,<sup>1</sup> Xinxing Zhou,<sup>1</sup> Hailu Luo,<sup>1, a)</sup> and Shuangchun Wen<sup>1, b)</sup>

Key Laboratory for Micro-/Nano-Optoelectronic Devices of Ministry of Education, College of Physics and Microelectronic Science, Hunan University, Changsha 410082, China

(Dated: 9 July 2014)

We present a simple and convenient method to yield cylindrical vector (CV) beams and realize its polarization evolution on higher-order Poincaré sphere based on inhomogeneous birefringent metasurface. By means of local polarization transformation of the metasurface, it is possible to convert a light beam with homogeneous elliptical polarization into a vector beam with any desired polarization distribution. The Stokes parameters of the output light are measured to verify our scheme, which show well agreement with the theoretical prediction. Our method may provide a convenient way to generate CV beams, which is expected to have potential applications in encoding information and quantum computation.

Cylindrical vector (CV) beams are light beams of which the polarization states are arranged with cylindrical symmetry in the beam cross section<sup>1</sup>. A plenty of unique properties originated from their special intrinsic symmetry have distinguished the CV beams from general optical beams with homogeneous polarization. For example, the radially polarized light, a subset of the CV beams, can lead to a strong longitudinal field in the case of strong focusing<sup>2,3</sup>. Because of these particularities, CV beams are expected with a broad applications such as particle trapping<sup>4</sup>, high resolution imaging<sup>2</sup>, particle acceleration<sup>5</sup>, and microscopy<sup>6</sup>.

Similar to the geometric representation of homogeneous polarizations on Poincaré sphere, a prominent geometric representation of the CV beams is provided by the so-called higher-order Poincaré sphere (HOPS)<sup>7,8</sup>. In this geometrical representation rule, higher-order Pancharatnam-Berry phase is demonstrated by cyclic transformation of the CV beams on the HOPS<sup>9,10</sup>. This phase is geometric in nature and differs significantly from a dynamic phase, which is proportional to light's total angular momentum. This state evolution will provide an advantage solution to create optical qubits, a single photon carrying several bits of information, which is expected to improve the flexibility of information encoding and simplify quantum computation<sup>11</sup>. Nevertheless, there is still not an effective method to generate all the states on HOPS and realize the state evolution. Most efforts including using subwavelength nanostructure<sup>12-14</sup>, orientation-tailored liquid crystal<sup>15-17</sup>, interferometry<sup>18,19</sup>, laser intracavity devices<sup>20</sup>, and fiber laser<sup>21,22</sup> have been made to obtain the radial and azimuthal polarized beams, however, the other states are seldom referred to.

In this work, we demonstrate a simple and convenient method to generate the CV beams and realize the evolution of polarization states on the HOPS. It is well known that the cascaded polarizer, quarter-wave plate (QWP), and half-wave plate (HWP) can generate any elliptical polarization state at will<sup>23</sup>. Furthermore, by modulating the direction of the optical axis of the QWP/HWP, the polarization can evolve

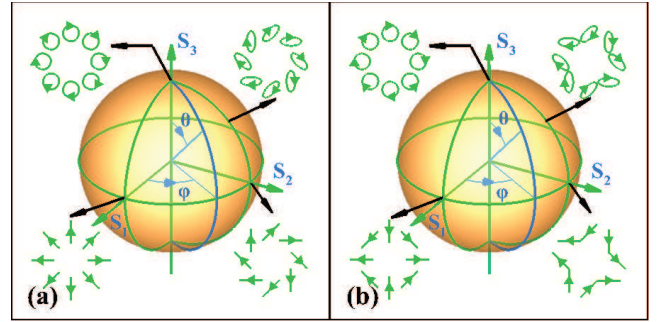


FIG. 1. Schematic illustration of the HOPS with (a)  $l = +1$  and (b)  $l = -1$ , respectively. The polarization distribution of four different points on each sphere are shown, and  $(\theta, \varphi)$  are the spherical coordinates of HOPS.

along the longitude/latitude on the surface of the fundamental Poincaré sphere. Analogously, while it comes to the CV beams whose polarization distribution are location-related, a special waveplate with space-variant optical axes should be employed. Fortunately, as a two dimensional electromagnetic nanostructure, metasurface with tailorable structure geometry possesses unparalleled advantages in optical phase<sup>24,25</sup> and polarization<sup>26</sup> manipulation, especially in subwavelength scale<sup>27-29</sup>, and is particularly amenable to produce and manipulate the CV beams.

We first consider the polarization transformation of a HWP with its fast and slow optical axes lying parallel to the  $xy$  coordinate plane. The Jones matrix of a HWP can be written as

$$\begin{pmatrix} \cos 2\Phi & \sin 2\Phi \\ \sin 2\Phi & -\cos 2\Phi \end{pmatrix}, \quad (1)$$

where  $\Phi$  is the orientation of the fast optical axis. Without loss of generality, a homogeneous elliptical polarization light is taken into account. It can be represented geometrically on the fundamental Poincaré sphere and algebraically described by the following equation in terms of the azimuthal and polar angles  $(\vartheta, \alpha)$  in the sphere,

$$|\psi(\vartheta, \alpha)\rangle = \cos\left(\frac{\vartheta}{2}\right)|R\rangle e^{i\sigma\frac{\alpha}{2}} + \sin\left(\frac{\vartheta}{2}\right)|L\rangle e^{-i\sigma\frac{\alpha}{2}}. \quad (2)$$

<sup>a)</sup>Electronic mail: hailuluo@hnu.edu.cn

<sup>b)</sup>Electronic mail: scwen@hnu.edu.cn

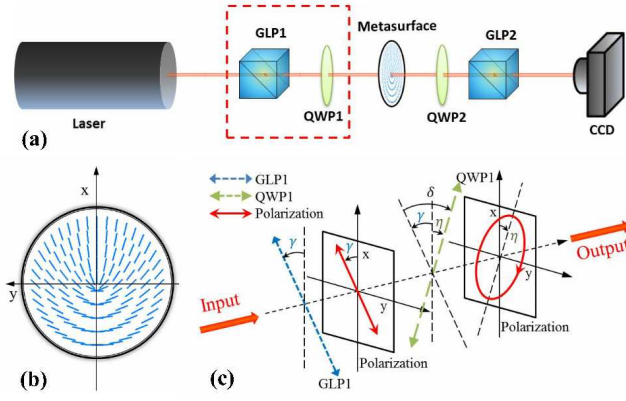


FIG. 2. (a) The experiment setup to generate CV beams. The He-Ne laser produces a linearly polarized light at 632.8nm wavelength (17 mW, Thorlabs HNL210L-EC). GLP, Glan laser polarizer; HWP, half waveplate; QWP, quarter waveplate; CCD, charge-coupled device (Coherent LaserCam HR). (b) Schematic drawing of the optical axes in metasurface. (c) The angular dependence of GLP, QWP, and the generated elliptical polarization.

Here  $|R\rangle = (\hat{x} + i\hat{y})/\sqrt{2}$  and  $|L\rangle = (\hat{x} - i\hat{y})/\sqrt{2}$  are respectively the right and left circular polarizations. The constant  $\sigma = \pm 1$  is associated with the spin angular momentum with  $\sigma\hbar$  per photon. When this beam impinges on the HWP at normal incidence, the resulting polarization is still elliptical with its polarization given by

$$|\psi(\vartheta', \alpha')\rangle = \cos\left(\frac{\vartheta'}{2}\right)|R\rangle e^{-i(\sigma\frac{\vartheta'}{2} + 2\Phi)} + \sin\left(\frac{\vartheta'}{2}\right)|L\rangle e^{i(\sigma\frac{\vartheta'}{2} + 2\Phi)}, \quad (3)$$

where  $\vartheta' = \pi - \vartheta$ ,  $\alpha' = -\alpha$ . It also represents an elliptical polarization located on the point  $(\vartheta', \alpha')$  of the fundamental Poincaré sphere. Actually, all the left-handed photons transform into right-handed photons and acquire an additional phase  $\exp(\pm 2\Phi)$ , and vice versa. As a result, the magnitude of the two components have also exchanged.

More interestingly, providing the HWP exhibits a space-variant optical axis direction, e.g.,  $\Phi = q\phi$  with  $\phi = \arctan(y/x)$  the local azimuthal angle and  $q$  is an integer or a semi-integer, the phase factor  $\exp(\pm 2\Phi)$  indicates an optical vortex with its topological charge  $l = \pm 2q$ . As the two orthogonal circular polarization components carry just opposite vortex phase, their coherent superposition actually forms a space-variant, inhomogeneous polarization beam, i.e., CV beam. In this case, Eq. (3) represents an arbitrary elliptical CV beam on the HOPS (see Fig. 1). This involves three free parameters  $\vartheta'$ ,  $\alpha'$ , and  $\Phi$ , which serve as effective ways to manipulate the CV beams. The first two parameters are related to the incident polarization which can be controlled by a polarizer and a QWP [see Fig. 2(a)]. As  $\Phi$  determines the topological charge, with different  $\Phi$ , the CV beams located on the HOPS with different topological charges  $l$ . Once the inhomogeneous HWP is manufactured, we can obtain any desired CV beam with a fixed topological charge and realize the polarization evolution on the HOPS.

We now can derive what kind of incident homogenous

polarization on the fundamental Poincaré sphere should be given, when a CV beam located on the point  $(\vartheta', \alpha')$  of the HOPS is desired. Comparing the Eq. (3) to (2), we can easily obtain the relationship:  $\vartheta = \pi - \vartheta'$  and  $\alpha = -\alpha'$ . However, in most cases, it is more effective to characterize the elliptical polarization with azimuth angle  $\eta$  and elliptical angle  $\delta$ . According to our calculation, the  $\eta$  and  $\delta$  of incident light can be associated with the spherical coordinates  $(\vartheta, \alpha)$  of HOPS in the forms,

$$\eta = \alpha' = -\alpha, \quad (4)$$

$$\delta = -\frac{1}{2}\left(\vartheta - \frac{\pi}{2}\right). \quad (5)$$

We implement an experiment to demonstrate this idea. The experimental apparatus is shown in Fig. 2(a). First, an elliptical polarization beam is produced by a polarizer (GLP1) and a quarter-wave plate (QWP1), and then passes through a inhomogeneous HWP. The inhomogeneous HWP now can be conveniently realized by an artificial inhomogeneous metasurface which is fabricated by etching space-variant grooves on a fused silica sample using a femtosecond laser<sup>13</sup>. This artificially creates an inhomogeneous form birefringence on the isotropic sample, and the local direction of the optical axes (slow and fast axes) are perpendicular and parallel to the grooves, respectively. This dielectric-based metasurface makes up a converter which can generate a CV beam when an elliptically polarized light is illuminated. To verify the viability of our scheme, we select a metasurface with  $q = 0.5$  and homogeneous  $\pi$  retardation (Altechna). Figure 2(b) shows the schematic drawing of the local optical axes. The Stokes parameters of the resulting beam is measured by a typical setup (QWP2, GLP2, and CCD).

By simply rotating the GLP1 or the QWP1, the azimuth angle or the ellipticity of the output elliptical polarization will change continuously, and we can get any elliptical polarization states from the first part of the setup, which is summarily illustrated in the Fig. 2(c). The azimuth angle  $\eta$  of the output polarization ellipse is the same as the optical axis direction of the QWP1 and the ellipticity angle  $\delta$  equals to the relative optical axis direction of the GLP1 and the QWP1. At the same time, the final state output from the metasurface will evolve on HOPS along the latitude or the longitude. In this way, we can generate arbitrary states on HOPS and realized the polarization state evolution on the HOPS.

To effectively analyze the emerging polarization states, we measured the Stokes parameters. They are a set of indices ( $S_0$ ,  $S_1$ ,  $S_2$ , and  $S_3$ ) that describe the polarization of light. When the optical axes of the QWP2 and polarizer (GLP2) make up the following combinations, what we get in the CCD camera are exactly the parameters<sup>30</sup>,

$$S_1 = I(0^\circ, 0^\circ) - I(90^\circ, 90^\circ), \quad (6)$$

$$S_2 = I(45^\circ, 45^\circ) - I(135^\circ, 135^\circ), \quad (7)$$

$$S_3 = I(-45^\circ, 0^\circ) - I(45^\circ, 0^\circ), \quad (8)$$

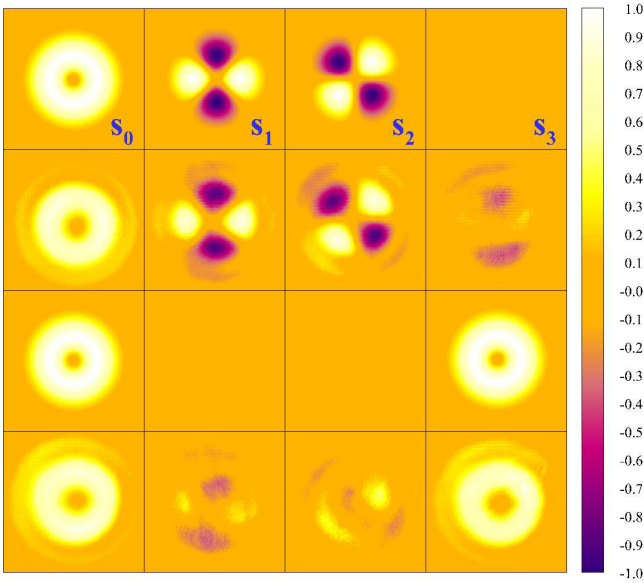


FIG. 3. Normalized Stokes parameters  $s_0$ ,  $s_1$ ,  $s_2$ , and  $s_3$ . The first and second rows are theoretical and experimental results of point the  $(1, 0, 0)$ , respectively. The third and fourth rows are the theoretical and experimental results corresponding to the point  $(0, 0, 1)$ . Both points are on the surface of the HOPS ( $l = +1$ ).

where  $I(\alpha, \beta)$  represents the intensity what we get when the optical axis of QWP2 is  $\alpha$  with the fixed  $x$  axis and the polarization direction of GLP2 is  $\beta$  with respect to the same  $x$  axis. The first Stokes parameter  $S_0$  is the intensity distribution of the output beam which can be recorded by the CCD without QWP2 and GLP2.

Figure 3 shows the normalized Stokes parameters  $s_i = S_i/S_0$  ( $i = 1, 2, 3$ ) of two points on the HOPS ( $l = +1$ ). It is known to all that  $s_1$  describes the linear polarization in  $x$  ( $s_1 = +1$ ) or  $y$  ( $s_1 = -1$ ) direction,  $s_2$  linear polarization in  $\pm 45^\circ$  ( $s_2 = \pm 1$ ) respect to the  $x$  direction, and  $s_3$  the degree of the circular polarization with  $s_3 = \pm 1$  corresponding to left- and right-handed polarization, respectively. Point  $(1, 0, 0)$  on the HOPS represents the radially polarization with axial symmetry [see Fig. 1(a)]. The  $s_1$  and  $s_2$  show a four-lobe pattern, with alternative  $+s_{1,2}$  and  $-s_{1,2}$  components. In this case  $s_3$  equals to 0, because the light beam is essential a linear polarization. While for point  $(0, 0, 1)$  which locates on the north pole of the HOPS, represents the circularly polarized vortex, so the  $s_{1,2} = 0$  and the  $s_3$  equals to the total intensity of the light ( $s_0$ ). In comparison with the theoretical distribution, the experimental results evidenced that the emerging beams are the desirable CV beams. For further verification, we mapped the polarization distribution. Firstly, we extracted the exact parameter values of any states from the Stokes parameters. Then, according to the relationship of the Stokes parameters and the polarization, the polarization states of the emerging beams are worked out. By depicting the graph of polarization distribution, we intuitively verify that the output beams are the desired CV beams. Figure 4 theoretically and experimentally record the polarization states of eight points on the

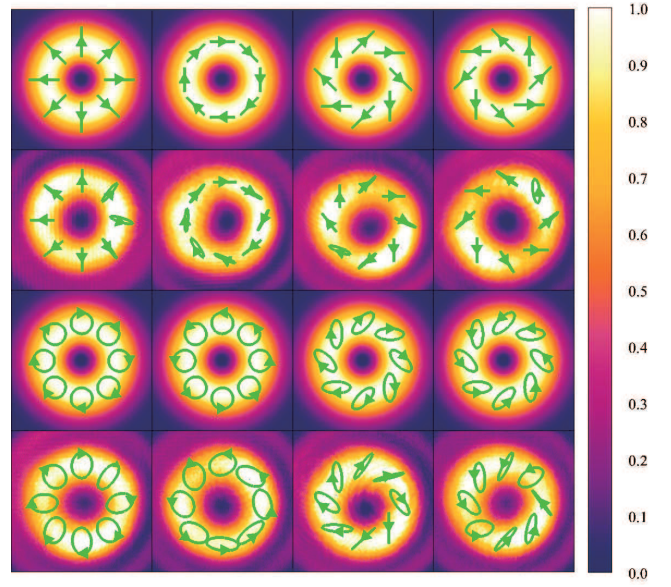


FIG. 4. The polarization and intensity distribution of the theoretical and experimental results. The first and second rows are respectively the theoretical and experimental results of the points  $(1, 0, 0)$ ,  $(-1, 0, 0)$ ,  $(0, 1, 0)$ , and  $(0, -1, 0)$  in the order from left to right. The third and fourth rows are the corresponding theoretical and experimental results of points  $(0, 0, 1)$ ,  $(0, 0, -1)$ ,  $(0, \sqrt{2}/2, \sqrt{2}/2)$ , and  $(0, \sqrt{2}/2, -\sqrt{2}/2)$ . All the points are on the surface of the HOPS ( $l = +1$ ).

HOPS ( $l = +1$ ). These points compose of two special paths on the sphere, one is on the equator and the other is on the longitude of azimuth angle  $\varphi = 45^\circ$ . Comparatively, the experimental results agree well with the theory. The deviation of the experimental results is because that, when extracting the parameter values, it is difficult to ensure the pictures located at the same pixel.

Although our experiments are limited to realizing the state evolution on HOPS with  $l = +1$ , our scheme is able to produce the states on HOPS with  $l = -1$  [Fig. 1(b)] and other larger  $|l|$ . It is well known that HWP would inverse the chirality of the passing light<sup>23</sup>. By inserting a HWP after the metasurface in our setup, we can change the sign of the topological charge. To generate vector beams with larger topological charge  $|l|$ , a metasurface with a larger  $q$  is needed. In general, it is theoretically possible to produce any states on all HOPSs, by inserting a HWP and a metasurface with suitable  $q$  values in our setup.

In conclusion, we have presented a simple and flexible method to produce arbitrary states on HOPS by using a birefringent metasurface. Within our setup, corresponding elliptical polarization can be converted to the desirable CV beam. The experimental results show well agreement with the theoretical ones, which is proved by measuring the Stokes parameters of the tested states. Furthermore, by simply rotating a GLP or QWP in our setup, the produced state will evolve along the latitude or longitude of the HOPS. It is believed that our scheme shall have potential applications in designing vector beams with more complex polarization distribution, encoding information, and quantum computation.

This research was partially supported by the National Natural Science Foundation of China (Grants Nos. 61025024, 11274106 and 11347120), and the Scientific Research Fund of Hunan Provincial Education Department of China (Grant No. 13B003).

- <sup>1</sup>Q. Zhan, *Adv. Opt. Photon* **1**, 1 (2009).
- <sup>2</sup>L. Novotny, M. R. Beversluis, K. S. Youngworth, and T. G. Brown, *Phys. Rev. Lett.* **86**, 5251 (2001).
- <sup>3</sup>R. Dorn, S. Quabis, and G. Leuchs, *Phys. Rev. Lett.* **91**, 233901 (2003).
- <sup>4</sup>Q. Zhan, *Opt. Express* **12**, 3377 (2004).
- <sup>5</sup>C. Varin and M. Piche, *Appl. Phys. B* **74**, S83 (2002).
- <sup>6</sup>A. F. Abouraddy and K. C. Toussaint, *Phys. Rev. Lett.* **96**, 153901 (2006).
- <sup>7</sup>A. Holleccek, A. Aiello, C. Gabriel, C. Marquardt, and G. Leuchs, *Opt. Express* **19**, 9714 (2011).
- <sup>8</sup>G. Milione, H. I. Sztul, D. A. Nolan, and R. R. Alfano, *Phys. Rev. Lett.* **107**, 053601 (2011).
- <sup>9</sup>M. V. Berry, *Proc. R. Soc. A* **392**, 45 (1984).
- <sup>10</sup>G. Milione, S. Evans, D. A. Nolan, and R. R. Alfano, *Phys. Rev. Lett.* **108**, 190401 (2012).
- <sup>11</sup>P. J. Leek, J. M. Fink, A. Blais, R. Bianchetti, M. Goppl, J. M. Gambetta, D. I. Schuster, L. Frunzio, R. J. Schoelkopf, and A. Wallra, *Science* **318**, 1889 (2007).
- <sup>12</sup>Z. Bomzon, V. Kleiner, and E. Hasman, *Appl. Phys. Lett.* **79**, 1587 (2001).
- <sup>13</sup>M. Beresna, M. Gecevičius, P. G. Kazansky, and T. Gertus, *Appl. Phys. Lett.* **98**, 201101 (2008).
- <sup>14</sup>K. Iwami, M. Ishii, Y. Kuramochi, K. Ida, and N. Umeda, *Appl. Phys. Lett.* **101**, 161119 (2012).
- <sup>15</sup>L. Marrucci, C. Manzo, and D. Paparo, *Phys. Rev. Lett.* **96**, 163905 (2006).
- <sup>16</sup>H. Chen, J. Hao, B. Zhang, J. Xu, J. Ding, and H. Wang, *Opt. Lett.* **36**, 3179 (2011).
- <sup>17</sup>X. Ling, X. Zhou, H. Luo, and S. Wen, *Phys. Rev. A* **86**, 053824 (2012).
- <sup>18</sup>X. Wang, J. Ding, W. Ni, C. Guo, and H. Wang, *Opt. Lett.* **32**, 3549 (2007).
- <sup>19</sup>U. Ruiz, P. Pagliusi, C. Provenzano, and G. Cipparrone, *Appl. Phys. Lett.* **102**, 116104 (2013).
- <sup>20</sup>R. Oron, S. Blit, N. Davidson, and A. A. Friesem, *Appl. Phys. Lett.* **77**, 3322 (2000).
- <sup>21</sup>M. Fridman, G. Machavariani, N. Davidson, and A. A. Friesem, *Appl. Phys. Lett.* **93**, 191104 (2008).
- <sup>22</sup>R. Zhou, B. Ibarra-Escamilla, J. W. Haus, P. E. Powers, and Q. Zhan, *Appl. Phys. Lett.* **95**, 191111 (2009).
- <sup>23</sup>J. N. Damask, *Polarization Optics in Telecommunications* (Springer, 2005).
- <sup>24</sup>X. Ni, A. V. Kildishev, and V. M. Shalaev, *Nat. Commun.* **4**, 2807 (2013).
- <sup>25</sup>L. Huang, X. Chen, H. Mühlenbernd, H. Zhang, S. Chen, B. Bai, Q. Tan, G. Jin, K. Cheah, C. Qiu, J. Li, T. Zentgraf, and S. Zhang, *Nat. Commun.* **4**, 2808 (2013).
- <sup>26</sup>X. Chen, L. Huang, H. Mühlenbernd, G. Li, B. Bai, Q. Tan, G. Jin, C. Qiu, S. Zhang, and T. Zentgraf, *Nat. Commun.* **3**, 1198 (2012).
- <sup>27</sup>N. Yu, P. Genevet, M. A. Kats, F. Aieta, J.-P. Tetienne, F. Capasso, Z. Gaburro, *Science* **334**, 333 (2011).
- <sup>28</sup>A. V. Kildishev, A. Boltasseva, V. M. Shalaev, *Science* **339**, 1232009 (2013).
- <sup>29</sup>N. Shitrit, I. Yulevich, E. Maguid, D. Ozeri, D. Veksler, V. Kleiner, E. Hasman, *Science* **340**, 724 (2013).
- <sup>30</sup>M. Born and E. Wolf, *Principles of Optics* (University Press, Cambridge, 1997).